Impact of secondary structure and hydration water on the dielectric spectrum of poly-alanine and possible relation to the debate on slaved versus slaving water

Klaus F. Rinne, Julius C. F. Schulz, and Roland R. Netz

Articles you may be interested in

Publisher's Note: "Impact of secondary structure and hydration water on the dielectric spectrum of poly-alanine and possible relation to the debate on slaved versus slaving water" [J. Chem. Phys. 142, 215104 (2015)]
J. Chem. Phys. **142**, 249901 (2015); 10.1063/1.4922998

Effect of temperature on the low-frequency vibrational spectrum and relative structuring of hydration water around a single-stranded DNA
J. Chem. Phys. **142**, 015101 (2015); 10.1063/1.4904896

Hydration shells of proteins probed by depolarized light scattering and dielectric spectroscopy: Orientational structure is significant, positional structure is not
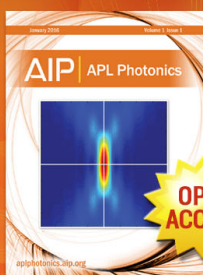J. Chem. Phys. **141**, 22D501 (2014); 10.1063/1.4895544

Depolarized light scattering and dielectric response of a peptide dissolved in water
J. Chem. Phys. **140**, 035101 (2014); 10.1063/1.4861965

Observation of high-temperature dynamic crossover in protein hydration water and its relation to reversible denaturation of lysozyme
J. Chem. Phys. **130**, 135101 (2009); 10.1063/1.3081137

Impact of secondary structure and hydration water on the dielectric spectrum of poly-alanine and possible relation to the debate on slaved versus slaving water

Klaus F. Rinne, Julius C. F. Schulz, and Roland R. Netz
Fachbereich Physik, Freie Universität Berlin, 14195 Berlin, Germany

Using extensive molecular dynamics simulations of a single eight-residue alanine polypeptide in explicit water, we investigate the influence of α-helix formation on the dielectric spectrum. For this, we project long equilibrium trajectories into folded and unfolded states and thereby obtain dielectric spectra representative for disordered as well α-helical conformations without the need to change any other system parameter such as pH or temperature. The absorption spectrum in the α-helical state exhibits a feature in the sub-GHz range that is significantly stronger than in the unfolded state. As we show by an additional decomposition into peptide and water contributions, this slow dielectric mode, the relaxation time of which matches the independently determined peptide rotational relaxation time, is mostly caused by peptide polarization correlations, but also contains considerable contributions from peptide-water correlations. In contrast, the peptide spectral contribution shows no features in the GHz range where bulk water absorbs, not even in the peptide-water correlation part, we conclude that hydration water around Ala$_8$ is more influenced by peptide polarization relaxation effects than the other way around. A further decomposition into water-self and water-collective polarization correlations shows that the dielectric response of hydration water is, in contrast to electrolyte solutions, retarded and that this retardation is mostly due to collective effects, the self relaxation of hydration water molecules is only slightly slowed down compared to bulk water. We find the dynamic peptide-water polarization cross correlations to be rather long-ranged and to extend more than one nanometer away from the peptide-water interface into the water hydration shell, in qualitative agreement with previous simulation studies and recent THz absorption experiments. © *2015 AIP Publishing LLC.* [http://dx.doi.org/10.1063/1.4921777]

I. INTRODUCTION

The dynamic interplay between a protein and its hydration water layer is argued to be of major importance for protein function, support for this view comes mostly from spectroscopy studies.[1–4] Spectra of protein solutions in electrolytes are typically separated into dispersive contributions at different time scales. For charged proteins, counter-ion diffusion causes relaxational processes in the sub-kHz range (the so-called α-process)[5,6] and the faster β-contribution is related to rotational peptide tumbling.[5–9] On the intermediate time scale between the β-process and the much faster bulk water relaxation in the GHz range (the so-called γ-process), a weak δ-dispersion has been seen, whose origin is somewhat unclear and which is controversially discussed.[7–10] Dielectric spectra of various proteins solvated in water have been measured as a function of the protein concentration[10–13] and the influence of the hydration shells on the dielectric signal has been estimated, based on the fact that hydration shells tend to overlap at higher concentrations. Simulation studies of small peptides as well as folded proteins helped to distinguish the spectral contributions from protein and hydration water and in particular elucidated the dynamic coupling between the protein and the surrounding water.[10,14–17]

In this paper, we are mostly interested in the effects of protein folding on the dielectric spectrum: for this, we introduce a dynamic projection formalism and compare the spectra of the folded and the unfolded peptide states and in particular investigate how the water hydration shell reacts to the conformational state of the peptide. Obtaining this information is in experiments for various reasons quite difficult: Bone[18] has measured the dielectric spectrum of β-lactamase solvated in water-urea mixtures at three different urea concentrations to study the effect of protein folding in 1994. He found an increase of the static dielectric constant from 98 to 121 by increasing the urea concentration from 0 to 4M and explained the growth by a higher number of absorbed water molecules in the unfolded state and a higher dipole moment of the denatured protein. Later, the dielectric spectrum of bovine serum albumin (BSA) has been measured for various urea concentrations.[19] The latter study considered that besides the protein unfolding at high urea concentrations, urea itself also modifies the dielectric spectrum. It turned out that the influence of urea on the dielectric spectra in the GHz range is stronger than the conformational change of the protein. In fact, aqueous urea solutions exhibit a pronounced spectral red shift with increasing urea concentration that has been observed in experiments[19] and molecular dynamics (MD) simulations[20]

and which is explained by a change of the water structure in the hydration shell around urea molecules. Due to the dominant spectral effects when using urea as a denaturant, it is generally difficult to investigate the difference of the protein spectral contribution in the native and unfolded states in such studies.

The protein conformational state can also be changed by varying the temperature. In recent experiments, a spectral blue shift has been observed for aqueous solutions of lysozyme with increasing temperature.[21] But since the water spectrum is temperature dependent itself,[22,23] the protein and water spectral effects are again difficult to disentangle.

Another way to induce protein folding or unfolding is to change the pH. Indeed, THz-absorption measurements of protein solutions at different pH values demonstrated pronounced differences between folded and unfolded structures,[15] but also here it should be noted that pH in the first place modifies the protein charge distribution which can affect the absorption properties independently from the protein conformational state.

In MD simulations, a direct way to separately obtain the spectra corresponding to folded and unfolded conformational substrates is to project a long equilibrium trajectory into sub-trajectories in the respective conformational subspaces. A similar projection has recently been used to obtain the IR spectrum of the large amylin protein from short simulation trajectories in different folding states.[24] Prerequisite for such a procedure is a separation of time scales, i.e., the simulation trajectory should be much longer than the typical folding/unfolding times which again should be much longer than the dominant polarization relaxation times (in fact, the scenario where the folding/unfolding time is of the order of the relaxation time of a polarization mode offers the additional opportunity to study dynamic interference effects, as will be briefly mentioned in Sec. IV). By employing such a projection procedure, which is further explained in Sec. II, we obtain the dielectric spectrum of poly-alanine Ala$_8$, which readily switches between an α-helical and a disordered conformation, in both conformational sub-ensembles, without the need to change temperature or any other system parameter. This very small model-peptide is ideal for the proof-of-principle of our dynamic projection formalism because the short folding time (of the order of $\tau_{\text{fold}} \approx 21$ ns as obtained in our simulations) allows to sample many folding/unfolding events in our simulation trajectories which have a total length of 7 μs, yet it is considerably longer than the peptide rotational relaxation of the order of $\tau_r \approx 800$ ps. A similar projection of protein spectra into folded and unfolded structures might in the future be possible experimentally by coupling spectroscopy with a second tool that allows to distinguish folded from unfolded states in real time (such as fluorescence resonance energy transfer (FRET) or circular dichroism); for this, high temporal resolution has to be achieved in single-molecule setups, which might be possible in the IR regime in the future.[25–27]

Our decomposition and projection method yields insights into the dynamic coupling between peptide motion and the surrounding water shell: while the polarization correlations between hydration water molecules themselves pick up a weak feature in the sub-GHz frequency range characteristic of the peptide relaxation mode, the peptide-peptide (PP) polarization shows no signal in the 10 GHz range, where bulk water polarizations relax. Even more remarkable, even the polarization correlations between the peptide and the hydration water are totally dominated by the sub-GHz relaxation representative of the peptide mode with no sign of fast water-like correlations. In connection to the literature debate on whether hydration water is slaved by the peptide dynamics or whether it slaves peptide dynamics,[1,2] we note that our data show no sign of the peptide acquiring any traces of fast water polarization dynamics, neither in the folded nor in the unfolded state. On the other hand, the dynamic polarization coupling between peptide and water is quite long-ranged and extends by more than one nanometer into the hydration shell, in agreement with recent theoretical and experimental findings.[3,4,16,28,29] Our conclusion is that while water certainly influences the peptide dynamics and determines the slowest peptide relaxation frequency via hydrodynamic friction effects on the reorientation dynamics, we do not see an effect of the water dielectric relaxation dynamics in the 10 GHz range on the peptide-peptide polarization spectrum. Our findings do not preclude alternative modes of water slaving that might not show up in the polarization in the GHz range or that need different or larger peptides than the short poly-alanine chain studied by us; certainly, our study shows the need for a more precise definition of the effects commonly described as dynamic water slaving.

II. METHODS

A. Dielectric response functions

The complex frequency-dependent dielectric susceptibility $\chi(f) = \chi'(f) - i\chi''(f)$ connects the total system polarization $\vec{P}(f)$ to the electric field $\vec{E}(f)$ via the linear-response relation $\vec{P}(f) = \chi(f)\epsilon_0\vec{E}(f)$, where ϵ_0 is the vacuum permittivity. According to the fluctuation dissipation theorem,[30,31] $\chi(f)$ follows from equilibrium polarization correlations via

$$\chi(f) = -\frac{1}{3Vk_BT\epsilon_0}\int_0^\infty e^{-2\pi i f t}\langle\vec{P}(0)\cdot\dot{\vec{P}}(t)\rangle \mathrm{d}t, \qquad (1)$$

where $\dot{\vec{P}}(t)$ denotes the time derivative of the time-dependent total polarization $\vec{P}(t)$, V is the system volume, and k_BT is the thermal energy. Via partial integration, Eq. (1) can be transformed into a form involving the polarization autocorrelation function $\phi(t) = \langle\vec{P}(0)\cdot\vec{P}(t)\rangle/(3Vk_BT\epsilon_0)$, which can be obtained easily from simulations

$$\chi(f) = \frac{\langle\vec{P}(0)\cdot\vec{P}(0)\rangle}{3Vk_BT\epsilon_0}$$
$$- \frac{i2\pi f}{3Vk_BT\epsilon_0}\int_0^\infty e^{-2\pi i f t}\langle\vec{P}(0)\cdot\vec{P}(t)\rangle \mathrm{d}t \qquad (2)$$

$$= \phi(0) - i2\pi f\int_0^\infty e^{-2\pi i f t}\phi(t)\mathrm{d}t. \qquad (3)$$

Since the end-capped Ala$_8$ employed in our simulations is charge neutral, our system contains no free charges and

the polarization $\vec{P}$ is independent of the origin. When free charges are present, ionic currents lead to additional spectral contributions, as demonstrated in our recent study on aqueous sodium-halide solutions.[32] In Subsections II B–II D, we introduce the projection and decomposition formalism in order to study the contributions of different components for the folded and unfolded states.

B. Projection into folded and unfolded states

In order to define whether the peptide at time t is folded or not, we use the root mean squared deviation $Q_{RMS}(t)$ of all alanine C_α-atoms from the ideal α-helical configuration. Other choices are possible, but are not expected to modify our results in a substantial way. A typical time evolution of $Q_{RMS}(t)$ is shown in Figure 1(a). The free energy landscape βF as a function of Q_{RMS} is shown in Figure 1(b). The projection operators $\Theta^f(t)$ and $\Theta^u(t) = 1 - \Theta^f(t)$ are defined to distinguish between folded and unfolded structures,

$$\Theta^f(t) = \begin{cases} 1, & \text{if } Q_{RMS}(t) < 0.166 \text{ nm} \\ 0, & \text{else} \end{cases}. \qquad (4)$$

The time-average of the projection operator of the folded state $\langle \Theta^f(t) \rangle_t = p^f = 1 - p^u = 0.75$ is identical to the probability to find the folded state p^f. The auto-correlation functions of the projection operators are shown in Figure 1(c) and are well described by a single exponential decay down to their long time limits $\langle \Theta^u(t) \rangle_t^2$ and $\langle \Theta^f(t) \rangle_t^2$ according to the following equations:

$$c^u(t) = \langle \Theta^u(0)\Theta^u(t) \rangle_t \qquad (5)$$

$$= e^{-t/\tau_{fold}} \langle (\Theta^u(t) - \langle \Theta^u(t) \rangle_t)^2 \rangle_t + \langle \Theta^u(t) \rangle_t^2 \qquad (6)$$

$$= p^u \left(e^{-t/\tau_{fold}} p^f + p^u \right), \qquad (7)$$

$$c^f(t) = \langle \Theta^f(0)\Theta^f(t) \rangle_t \qquad (8)$$

$$= e^{-t/\tau_{fold}} \langle (\Theta^f(t) - \langle \Theta^f(t) \rangle_t)^2 \rangle_t + \langle \Theta^f(t) \rangle_t^2 \qquad (9)$$

$$= p^f \left(e^{-t/\tau_{fold}} p^u + p^f \right), \qquad (10)$$

where the equations fulfil the relation $\partial c^u(t)/\partial t = \partial c^f(t)/\partial t$ and where the time constant $\tau_{fold} = 20.9$ ns (fitted to the data in Figure 1(c)) is a measure for the transition time. Since τ_{fold} is much longer than the polarization relaxation times which are of the order of hundreds of picoseconds, the folding/unfolding dynamics do not affect our spectral results, which are mostly located in the GHz range. Dielectric spectroscopy measurements in the kHz-MHz regime might in the future be able to see a mode related to the folding/unfolding dynamics.

Using the projection operator, we decompose the polarization correlation functions and the spectral signal according to the peptide secondary structure into folded and unfolded contributions,

$$\phi^f(t) = \langle \Theta^f(0)\vec{P}(0) \cdot \vec{P}(t) \rangle / (3V k_B T \epsilon_0 p^f), \qquad (11)$$

$$\phi^u(t) = \langle \Theta^u(0)\vec{P}(0) \cdot \vec{P}(t) \rangle / (3V k_B T \epsilon_0 p^u), \qquad (12)$$

$$\phi(t) = p^f \phi^f(t) + p^u \phi^u(t), \qquad (13)$$

$$\chi^f(f) = \phi^f(0) - i2\pi f \int_0^\infty e^{-2\pi i f t} \phi^f(t) dt, \qquad (14)$$

$$\chi^u(f) = \phi^u(0) - i2\pi f \int_0^\infty e^{-2\pi i f t} \phi^u(t) dt, \qquad (15)$$

$$\chi(f) = p^f \chi^f(f) + p^u \chi^u(f). \qquad (16)$$

Note that we use a single projection in the autocorrelation function, which is warranted since the folding times are substantially longer than the typical polarization relaxation times we are interested in (i.e., polarization cross correlations between folded and unfolded states are insignificant, as we explicitly checked). Thus, $\phi^f(t)$ is equal to the polarization autocorrelation function of a permanently folded system for times up to the order of $\tau_{fold} \approx 21$ ns, above which a conformational change becomes likely. As a consequence, the spectral signal $\chi^f(f)$ is identical to the spectrum of a permanently folded system in the frequency range from 100 MHz to 1 THz as covered in our study.

C. Decomposition into water, peptide, and self and collective contributions

In the absence of free charges, the polarization $\vec{P}$ of a peptide solution consists of the water polarization $\vec{P}_W$ and the peptide polarization $\vec{P}_P$ according to $\vec{P} = \vec{P}_W + \vec{P}_P$. The water polarization $\vec{P}_W$ can be split into the polarization of the hydration shell water $\vec{P}_H$ and the remaining outer shell water $\vec{P}_O = \vec{P}_W - \vec{P}_H$. Water molecules, whose oxygen atoms have a
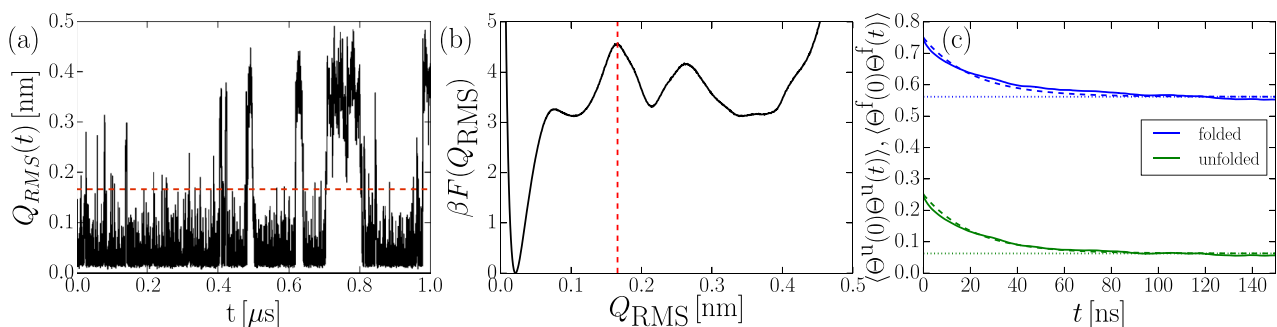

FIG. 1. (a) Typical time evolution of the root mean squared deviation $Q_{RMS}(t)$ of Ala$_8$ from the ideal α-helix. (b) Free energy landscape βF as a function of Q_{RMS}. The dashed red lines in (a) and (b) denote the threshold $Q_{RMS} = 0.166$ nm used to distinguish folded from unfolded states. (c) Auto-correlation functions of the unfolded and folded projection operators Θ^u (green) and Θ^f (blue). The dashed lines are exponential fits with a decay time $\tau_{fold} = 20.9$ ns according to Eqs. (6) and (9) and the dotted horizontal lines denote the long time limits.

distance of less than $R_H = 3$ Å from the nearest peptide atom, are denoted as hydration shell water. We use this relatively low threshold in most of our data analysis, in order to concentrate on the dominant effects in the first hydration shell. As a matter of fact, the dynamic influence of the peptide on the solvation water extends much further than 3 Å, as we discuss further below, in accordance with experimental and simulation results.[3,4,16,28,29] Note that due to our relatively small simulation box, dictated by the need to perform very long simulations, the dynamics in the outer hydration shells is still quite different from bulk water, as we will discuss further below. The partitioning of water molecules into hydration water and outer-shell water is done according to the closest distance between a water molecule and the periodically replicated peptide molecule, which renders a non-ambiguous definition of the hydration distance. Defining the cross correlation functions between the various polarization components and the total polarization as

$$\phi_W(t) = \frac{\langle \vec{P}_W(0) \cdot \vec{P}(t) \rangle}{3Vk_BT\epsilon_0}, \qquad (17)$$

$$\phi_H(t) = \frac{\langle \vec{P}_H(0) \cdot \vec{P}(t) \rangle}{3Vk_BT\epsilon_0}, \qquad (18)$$

$$\phi_O(t) = \frac{\langle \vec{P}_O(0) \cdot \vec{P}(t) \rangle}{3Vk_BT\epsilon_0}, \qquad (19)$$

$$\phi_P(t) = \frac{\langle \vec{P}_P(0) \cdot \vec{P}(t) \rangle}{3Vk_BT\epsilon_0}, \qquad (20)$$

we can express the spectral contribution of each system component as

$$\chi_W(f) = \phi_W(0) - i2\pi f \int_0^\infty e^{-2\pi ift} \phi_W(t)dt, \qquad (21)$$

$$\chi_H(f) = \phi_H(0) - i2\pi f \int_0^\infty e^{-2\pi ift} \phi_H(t)dt, \qquad (22)$$

$$\chi_O(f) = \phi_O(0) - i2\pi f \int_0^\infty e^{-2\pi ift} \phi_O(t)dt, \qquad (23)$$

$$\chi_P(f) = \phi_P(0) - i2\pi f \int_0^\infty e^{-2\pi ift} \phi_P(t)dt. \qquad (24)$$

Accordingly, the total polarization auto-correlation function $\phi(t)$ as well as the total susceptibility $\chi(f)$ can be expressed as sums over different contributions

$$\phi(t) = \phi_W(t) + \phi_P(t) \qquad (25)$$

$$= \phi_H(t) + \phi_O(t) + \phi_P(t), \qquad (26)$$

$$\chi(f) = \chi_W(f) + \chi_P(f) \qquad (27)$$

$$= \chi_H(f) + \chi_O(f) + \chi_P(f). \qquad (28)$$

In addition, we define the cross correlation between the polarization of components k and l as

$$\phi_{k\,l}(t) = \frac{\langle \vec{P}_k(0) \cdot \vec{P}_l(t) \rangle}{3Vk_BT\epsilon_0}, \qquad (29)$$

where k and l can represent protein P, total water W, hydration shell water H, or outer shell water O. So, for instance, the polarization cross correlation between hydration shell water (H) at time zero and outer shell water (O) at time t is

$$\phi_{HO}(t) = \frac{\langle \vec{P}_H(0) \cdot \vec{P}_O(t) \rangle}{3Vk_BT\epsilon_0}, \qquad (30)$$

where the respective spectral contributions are given analogously to Eqs. (21)–(24) and the total spectra consist of three, four, or six terms depending on the level of decomposition

$$\chi(f) = \chi_{WW}(f) + \chi_{PP}(f) + 2\chi_{WP}(f) \qquad (31)$$

$$= \chi_{HW}(f) + \chi_{OW}(f) + \chi_{PP}(f) + 2\chi_{WP}(f) \qquad (32)$$

$$= \chi_{HH}(f) + \chi_{OO}(f) + \chi_{PP}(f) + 2\chi_{HO}(f) + 2\chi_{HP}(f) + 2\chi_{OP}(f). \qquad (33)$$

The water contributions WW, HW, and OW are further decomposed into self and collective correlations. We only write down the definition for the hydration shell water here; as for outer shell water and the total water contributions, the definitions are analogous,

$$\phi_{HW,self}(t) = \frac{1}{3Vk_BT\epsilon_0} \sum_{i\in\{N_H\}} \langle \vec{p}_i(0) \cdot \vec{p}_i(t) \rangle, \qquad (34)$$

$$\phi_{HW,coll}(t) = \frac{1}{3Vk_BT\epsilon_0} \sum_{i\in\{N_H\}} \sum_{j\neq i}^N \langle \vec{p}_i(0) \cdot \vec{p}_j(t) \rangle, \qquad (35)$$

where $\{N_H\}$ is the ensemble of hydration shell water and $N = 688$ is the total number of water molecules. By construction, the sum over the self and collective terms returns the polarization cross correlation function between hydration shell water and the total water ensemble,

$$\phi_{HW}(t) = \phi_{HW,self}(t) + \phi_{HW,coll}(t). \qquad (36)$$

The decomposed spectral contributions follow as

$$\chi_{HW,self}(f) = \phi_{HW,self}(0) - i2\pi f \int_0^\infty e^{-2\pi ift} \phi_{HW,self}(t)dt, \qquad (37)$$

$$\chi_{HW,coll}(f) = \phi_{HW,coll}(0) - i2\pi f \int_0^\infty e^{-2\pi ift} \phi_{HW,coll}(t)dt. \qquad (38)$$

In principle, the spectral contributions of all different components can be further projected into the folded and unfolded states analogously to Eqs. (11)–(16) to generate projected polarization correlation functions $\phi_{kl}^f(t)$ and $\phi_{kl}^u(t)$ and the corresponding spectral contributions $\chi_{kl}^f(f)$ and $\chi_{kl}^u(f)$. Needless to say, we will only present a limited number of data in this paper, carefully selected to highlight the most interesting features of the system we studied.

D. Simulations methods

We use GROMACS 4.5.4[33] and perform seven simulation runs each of length 1 μs for an end-capped eight-residue alanine (Ala$_8$) in a rhombic dodecahedron of mean volume 21.4 nm^3, yielding a mean distance of 3.1 nm between the peptide and its periodic images, solvated in 688 SPC/E[51] water

molecules in the NPT ensemble at 300 K and atmospheric pressure. The amber03 force field,[34] the GROMACS v-rescale thermostat,[35] a Parrinello-Rahman barostat,[36] and a 2 fs integration time step are used. The neighbor list is updated every 20 fs and the trajectories are collected every 100 fs. The electrostatics are computed by particle mesh Ewald methods and the Lennard-Jones interactions are cutoff at 0.9 nm. Because of memory limitations, all trajectories are split in segments of 200 ns length for data analysis. The polarization components of each segment are Fourier transformed via Fast Fourier Transformation (FFT) and correlations are calculated by multiplication in Fourier space. After back transformation into the time domain, the correlation functions are averaged over all segments. A time cutoff is used during calculation of the spectra via Laplace transformation of the correlation functions, so that the correlation functions are only integrated up to the time, where they first drop below zero. For the calculation of the polarization correlation functions, we update the decomposition of water into different solvation shells every 100 fs according to the current configuration; consequently, the water partitioning changes in time. For the calculation of the self polarization correlations, the trajectories are split in segments of 1 ns length. The dipolar auto-correlation function of each water molecule is calculated and then clustered into the different solvation shells depending on the water configuration at the beginning of each trajectory segment. One nanosecond is sufficiently long to obtain correlations in the relevant time range, since the

single dipole auto-correlation function drops below zero within 300 ps in our simulations. The collective correlations become negative within 3 ns and are obtained by subtracting the self correlation from the total water polarization correlations. The peptide polarization auto-correlation function ϕ_{PP} becomes negative at about 6 ns.

III. RESULTS

A. Spectral fits

For a quantitative analysis, we fit a Cole-Cole function according to

$$\chi(f) = \frac{\epsilon}{1 + (i\,2\pi f \tau)^{1-\alpha}} + \chi_\infty \qquad (39)$$

to the different spectral components with the fit parameters $\epsilon, \tau, \alpha,$ and χ_∞. We do not set $\chi_\infty = 0$, since for some components, the real part of the high frequency susceptibility does not vanish due to integration errors caused by the finite time resolution of our data of 100 fs. We fit the real and imaginary parts of the dielectric spectra simultaneously with the error functional $(\Delta\chi')^2 + (2\Delta\chi'')^2$ using a logarithmic distribution of sample frequencies in the range between 0.1 and 100 GHz. We restrict the fitting range up to 100 GHz, since the high frequencies are more prone to integration errors due to the rather long sampling period of 100 fs. In order to roughly

TABLE I. Cole-Cole fit parameters for the total spectrum $\chi(f)$ and all spectral contributions. Contributions involving the peptide (P) show a long relaxation time, which is even slower when the peptide is folded. H denotes hydration water, while O denotes the remaining outer shell water. The total water ensemble is labelled by W. Collective water relaxations (coll) in general have slower relaxation times than self relaxations (self). The values for pure bulk water χ_{bulk} are taken from our previous work.[37] The Cole-Cole exponent α, which indicates departures from a single-Debye form, is particularly large for the total spectrum $\chi(f)$ and the hydration water contributions $\chi_H(f)$ and $\chi_{HH}(f)$. For these contributions, multiple Debye fits are also performed and presented in Tables II and III.

	ϵ	ϵ^{f}	ϵ^{u}	τ (ps)	τ^{f} (ps)	τ^{u} (ps)	α	α^{f}	α^{u}	χ_∞
Total χ	72.63	74.36	67.80	12.04	12.12	11.82	0.122	0.145	0.047	−1.42
χ_P	5.83	7.00	2.43	715.37	730.82	538.08	0.037	0.024	0.187	0.07
χ_W	66.85	67.25	65.40	11.72	11.71	11.75	0.041	0.047	0.021	1.01
χ_O	62.38	62.55	61.16	11.51	11.53	11.56	0.030	0.030	0.018	1.24
χ_H	4.76	4.90	4.49	17.12	18.16	15.20	0.261	0.315	0.105	−0.35
χ_{PP}	3.85	4.70	1.35	719.14	734.18	550.03	0.025	0.014	0.161	0.07
χ_{WP}	1.96	2.21	1.09	702.63	699.08	543.34	0.051	0.018	0.224	0.01
χ_{OP}	1.23	1.40	0.72	674.26	684.39	531.32	0.040	0.014	0.220	0.00
χ_{HP}	0.70	0.82	0.36	723.88	739.21	576.78	0.039	0.020	0.232	0.01
χ_{WW}	65.11	65.17	64.95	11.64	11.62	11.71	0.018	0.019	0.016	1.71
$\chi_{WW,self}$	16.12	15.39	18.30	5.13	5.13	5.13	0.048	0.048	0.048	1.86
$\chi_{WW,coll}$	50.85	51.91	47.69	14.19	14.10	14.35	−0.012	−0.001	−0.042	−1.35
χ_{OW}	62.92	63.37	61.27	11.56	11.55	11.58	0.037	0.042	0.019	1.04
$\chi_{OW,self}$	15.31	14.61	17.37	5.12	5.13	5.12	0.048	0.048	0.048	1.77
$\chi_{OW,coll}$	47.79	48.88	44.42	13.95	13.85	14.14	−0.015	−0.005	−0.045	−1.24
χ_{HW}	3.89	3.80	4.13	15.21	15.46	14.66	0.081	0.091	0.042	−0.00
$\chi_{HW,self}$	0.82	0.78	0.94	5.25	5.24	5.25	0.054	0.054	0.054	0.09
$\chi_{HW,coll}$	3.08	3.03	3.22	18.63	18.97	17.61	0.024	0.036	−0.019	−0.13
χ_{HO}	2.58	2.53	2.73	17.47	17.70	16.71	0.007	0.015	−0.022	−0.40
χ_{OO}	58.77	58.96	58.29	11.25	11.24	11.29	0.014	0.014	0.017	2.03
χ_{HH}	1.36	1.32	1.45	9.16	9.19	9.17	0.214	0.236	0.154	0.33
χ_{bulk}	70.92			10.72			0.014			
$\chi_{bulk,self}$	18.78			4.32			0.122			
$\chi_{bulk,coll}$	51.95			12.96			−0.074			

TABLE II. Double Debye fit parameters for the total spectrum and the contributions involving water in the first hydration shell (H). These spectra consist of a fast bulk water-like process and a separate much slower process. χ_{HH} is due to auto-correlations of the hydration shell water, χ_{HO} denotes the cross correlations between hydration water and the remaining outer shell water, $\chi_{HW} = \chi_{HH} + \chi_{HO}$ denotes the correlations between hydration water and the total water ensemble. $\chi_{HW,coll}$ denotes the collective part of χ_{HW}.

	χ	χ_{HH}	χ_{HO}	χ_{HW}	$\chi_{HW,coll}$
ϵ_1	8.61	0.17	0.21	0.37	0.33
ϵ_1^f	10.27	0.18	0.24	0.41	0.38
ϵ_1^u	3.74	0.71	0.13	0.26	0.20
ϵ_2	63.84	1.06	2.53	3.55	2.96
ϵ_2^f	63.75	1.02	2.46	3.42	2.87
ϵ_2^u	63.73	0.66	2.76	3.89	3.24
τ_1 (ps)	604.65	195.94	1047.21	548.63	1041.31
τ_1^f (ps)	634.62	286.77	1029.34	592.95	1038.51
τ_1^u (ps)	332.67	17.88	1043.47	339.24	1132.76
τ_2 (ps)	11.61	8.77	16.97	14.55	17.81
τ_2^f (ps)	11.57	9.01	17.05	14.64	17.94
τ_2^u (ps)	11.60	4.72	16.65	14.23	17.48
χ_∞	2.32	0.47	−0.41	0.12	−0.12

TABLE III. Triple Debye fit parameters for the spectral contribution χ_{HH} of the polarization auto-correlation of hydration shell water.

	ϵ_1	ϵ_2	ϵ_3	τ_1 (ps)	τ_2 (ps)	τ_3 (ps)	χ_∞
χ_{HH}	0.14	0.83	0.35	577.77	13.23	2.94	0.40
χ_{HH}^f	0.15	0.80	0.33	625.18	13.36	2.94	0.39
χ_{HH}^u	0.10	0.96	0.38	360.03	12.47	2.87	0.43

Cole-Cole fits. Here, we perform double Debye fits according to

$$\chi(f) = \frac{\epsilon_1}{1 + i\,2\pi f\,\tau_1} + \frac{\epsilon_2}{1 + i\,2\pi f\,\tau_2} + \chi_\infty, \qquad (40)$$

which drastically improves the fitting quality. The results of these fits are listed in Table II and we will refer to them in Secs. III B–III D. The spectral contribution χ_{HH} cannot even be well reproduced by a double Debye fit (fit not shown). Here, we perform a triple Debye fit according to

$$\chi(f) = \frac{\epsilon_1}{1 + i\,2\pi f\,\tau_1} + \frac{\epsilon_2}{1 + i\,2\pi f\,\tau_2} + \frac{\epsilon_3}{1 + i\,2\pi f\,\tau_3} + \chi_\infty,$$

with the fit parameters listed in Table III.

B. Total spectrum

In Figure 2, we present the real (a) and imaginary (d) parts of the total dielectric spectrum for the entire trajectory including unfolded and folded sections (black line), as well as for the projected folded (blue line) and unfolded contributions (green line). A second absorption peak in the sub-GHz range appears in addition to the bulk water resonance around 10 GHz

achieve the same relative errors for real and imaginary parts, we use a higher weight for the imaginary part, since it has a lower absolute value. The resulting Cole-Cole fit parameters are listed for all states and contributions in Table I and are discussed in Secs. III B–III D.

As will be discussed later on in more detail, some spectra, in particular the total spectrum χ as well as the contributions χ_{HH}, χ_{HO}, χ_{HW}, and $\chi_{HW,coll}$, are not well described by
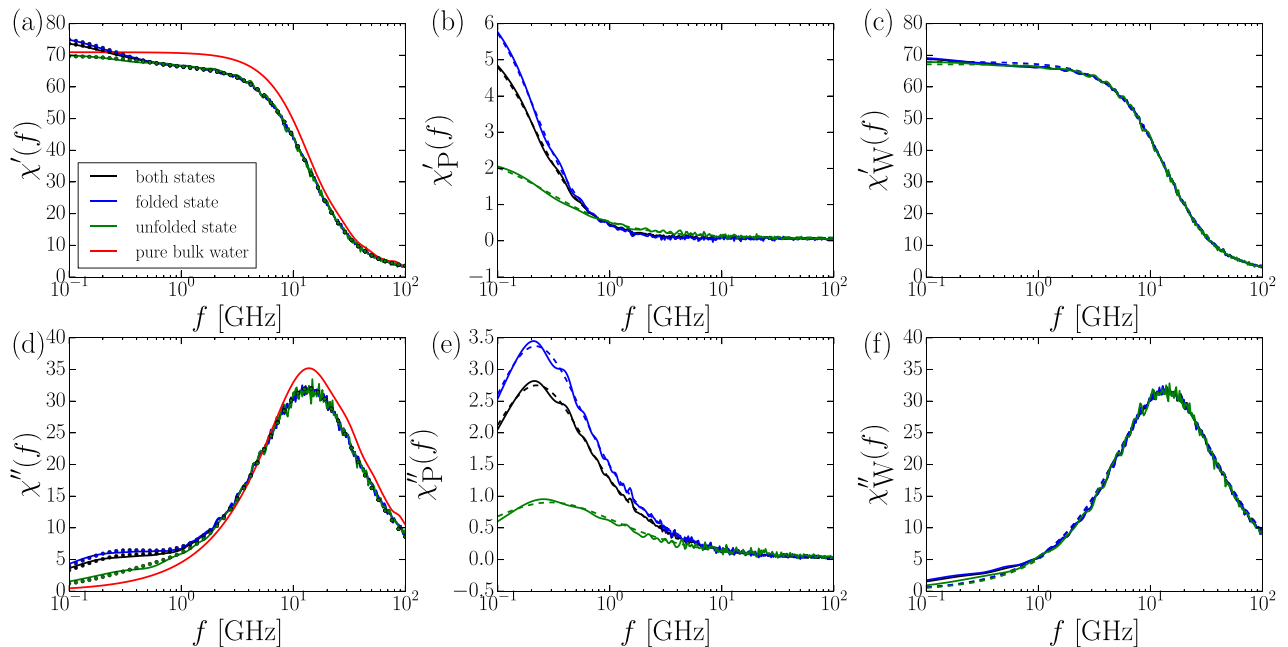

FIG. 2. The real (a) and imaginary (d) parts of the total dielectric susceptibility $\chi(f)$ for folded (blue), unfolded (green), and entire trajectories (black lines). The spectra from simulations of pure water are included for comparison (red lines). The low frequency shoulder around 200 MHz is more pronounced in the folded state, but also visible in the unfolded state. The real (b) and imaginary (e) parts of the peptide contribution $\chi_P(f)$ are much stronger in the folded state (blue lines) compared to the unfolded state (green lines) and show no feature at the water relaxation frequency around 10 GHz. The water contribution $\chi_W(f)$ (c) and (f) shows only a relatively weak dependence on the secondary structure in the sub-GHz range. Solid lines denote simulation data, dotted lines in (a) and (d) denote double Debye fits, and dashed lines in (b) and (e) and (c) and (f) are Cole-Cole fits. Note that according to our decomposition scheme, $\chi(f) = \chi_W(f) + \chi_P(f)$.
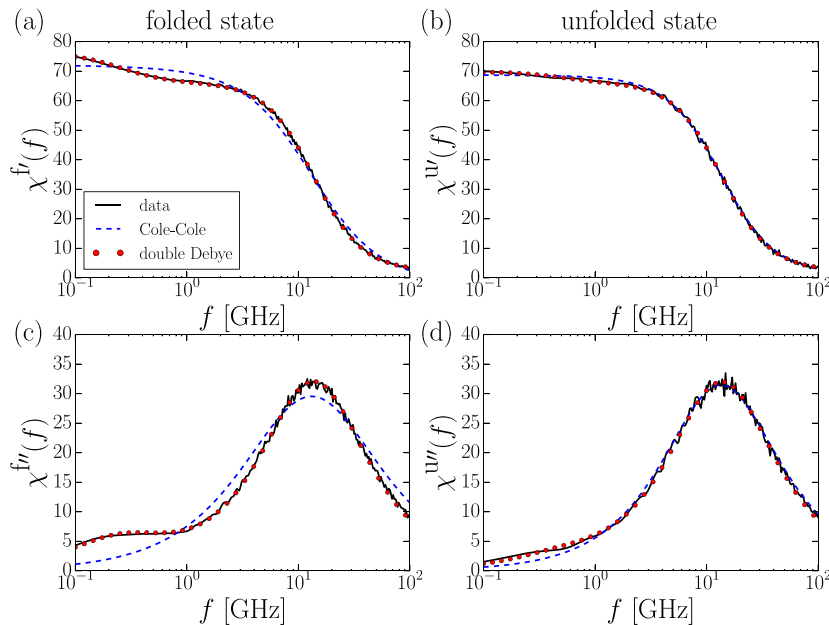
FIG. 3. Comparison of Cole-Cole (blue dashed lines) and double Debye fits (red dots) to the total spectrum $\chi(f)$ (black solid lines) in the folded (a) and (c) and unfolded states (b) and (d). Especially for the folded state, the Cole-Cole fit is not applicable.

(the red line shows the spectrum of a simulation of pure water for comparison), this slow contribution is more significant in the folded state. A double Debye fit describes the spectrum in the folded state very well (dotted lines), yielding relaxation times of 11.6 ps and 635 ps (see Table II for all double-Debye fit parameters). On the other hand, a single Cole-Cole fit cannot describe the data in the unfolded or folded states, as demonstrated in Figure 3. The low frequency absorption is mainly caused by the peptide contribution $\chi_P(f)$ and is much stronger if the peptide is folded, as shown in Figures 2(b) and 2(e). On the other hand, the influence of the secondary structure on the water absorption $\chi_W(f)$ is quite weak, as shown in Figures 2(c) and 2(f): we see a slight shoulder in the sub-GHz range, which is particularly noticeable when looking at the deviations between the simulation data (solid lines) from the Cole-Cole fits (broken lines, note that the three fits for the entire trajectory and the projections into folded and unfolded states basically overlap), and this shoulder is more pronounced in the folded state (blue line). Interestingly, we do not see a spectral contribution at the water relaxation frequency around

10 GHz in $\chi_P(f)$ and only a weak spectral contribution at the dominant peptide relaxation frequency around 200 MHz in $\chi_W(f)$; so, based on our analysis, a slaving influence of water on the peptide polarization relaxation is not detectable and water is only weakly slaved by the peptide dynamics, both in the unfolded and in the folded states, which is interesting in the light of extensive literature discussions on this matter.[1,2] We will come back to this point in Sec. IV.

C. Peptide contribution

We first have a closer look on the peptide absorption signal. In Figure 4(a), we present a two-dimensional plot of the Ala$_8$ peptide probability density distribution ρ as a function of the root mean squared deviation from the ideal α-helix, Q_{RMS}, and the static peptide dielectric susceptibility contribution, which is proportional to the square of the peptide dipole moment, $\chi'_{PP}(f=0) = |\vec{P}_P^2|/(3Vk_BT\epsilon_0)$. The highest local probability is obtained for folded states in connection with a high peptide polarization and a second local maximum
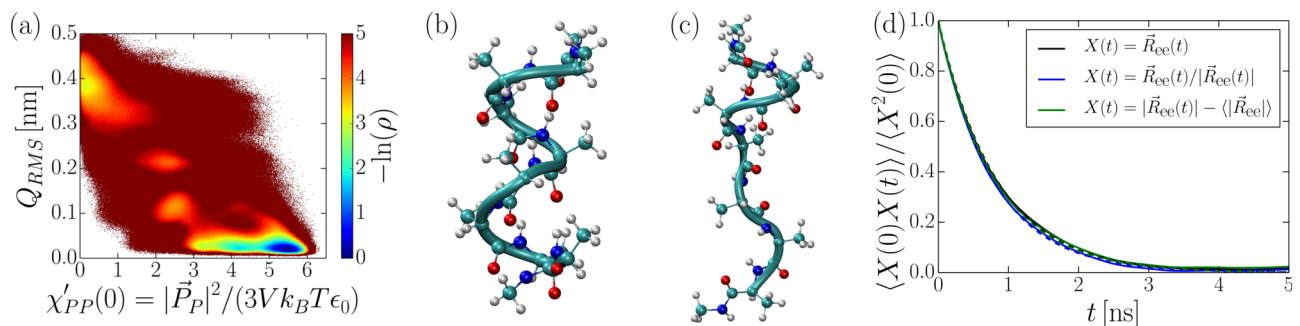

FIG. 4. (a) Two-dimensional probability density landscape as a function of the root mean squared deviation Q_{RMS} of Ala$_8$ from the ideal α-helix and the static dielectric peptide susceptibility $\chi'_{PP}(0) = |\vec{P}_P^2|/(3Vk_BT\epsilon_0)$. (b) Snapshot of an α-helical Ala$_8$ structure: the negatively charged oxygens (red) point down, while the positively charged nitrate groups (nitrogen is colored in blue) point upwards. As a consequence, this configuration has a high dipole moment pointing upwards. (c) Snapshot of an unfolded structure. (d) Auto-correlation function of the end-to-end vector $\vec{R}_{ee}$ (black), the end-to-end unit vector $\vec{R}_{ee}/|\vec{R}_{ee}|$ (blue), and the magnitude of the end-to-end vector $|\vec{R}_{ee}(t)| - \langle|\vec{R}_{ee}|\rangle$ (green), obtained from the entire trajectory. All three correlation functions decay exponentially with decay times of about 800 ps (dashed lines).
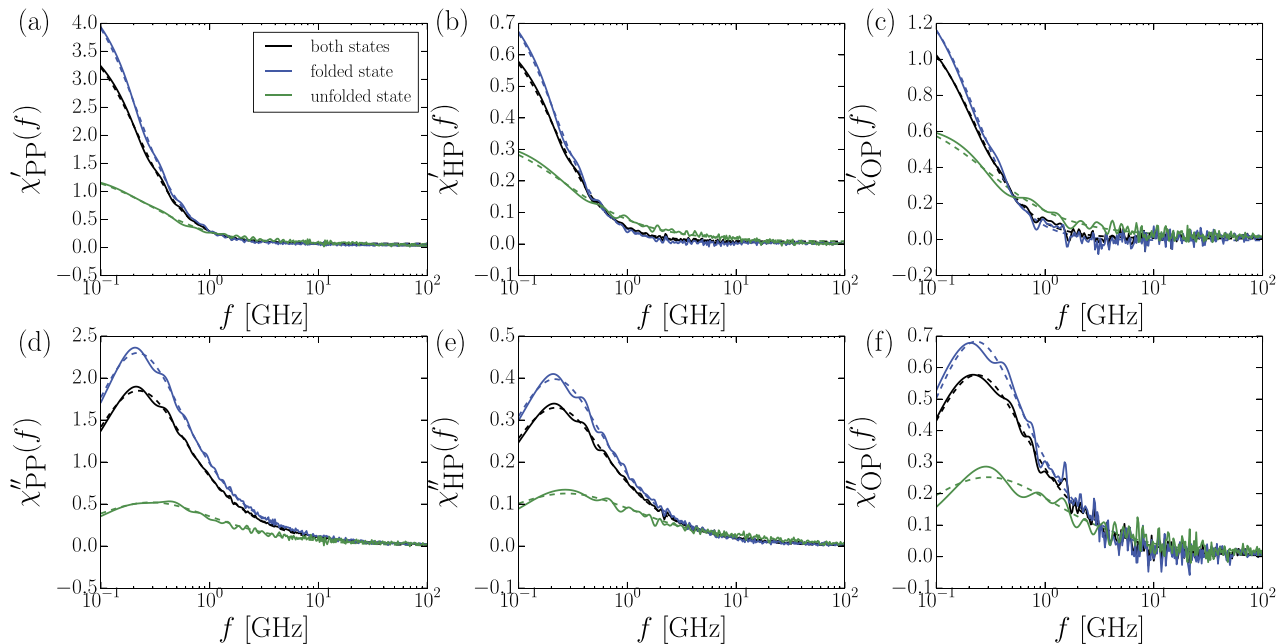
FIG. 5. Real (a) and imaginary (d) parts of the peptide-peptide dielectric susceptibility contribution $\chi_{PP}(f)$ in the folded state (blue), the unfolded state (green), and for the entire trajectory (black lines). The dominant response appears in the sub-GHz range and is much stronger if the peptide is folded. The peptide-hydration-water cross correlation $\chi_{HP}(f)$ (b) and (e) and peptide-outer shell-water cross correlation $\chi_{OP}(f)$ (c) and (f) have very similar shape. No features at frequencies corresponding to water polarization correlations around 10 GHz are seen. Note that $\chi_{PP} + \chi_{HP} + \chi_{OP} = \chi_P$. Broken lines denote Cole-Cole fits.

appears for unfolded states with a weak peptide polarization. A snapshot of the folded state in Figure 4(b) illustrates the high polarization of the peptide, since the negatively charged oxygen atoms (red) point all down, while the positively charged nitrate groups (nitrogen is colored in blue) point upwards. Since the strong polarization is caused by the peptide backbone and not the side chains, it transpires that α-helical peptides in general show similar effects, regardless of their sequence and side-chain composition. The snapshot of an unfolded state in Figure 4(c) indicates much less polarization.

Boresch $et\ al.$[14] have previously further decomposed the spectral peptide contribution χ_P for single-alanine and di-alanine solutions into the peptide auto-contribution χ_{PP} and peptide cross terms with the hydration water χ_{HP} and the remaining outer shell water χ_{OP}. They have shown that all these contributions have almost identical relaxation times and that the relaxation time increases from single-alanine to di-alanine. We show the three contributions χ_{PP}, χ_{HP}, and χ_{OP} in Figure 5; note that the sum $\chi_{PP} + \chi_{HP} + \chi_{OP} = \chi_P$ equals the peptide contribution previously discussed and shown in Figures 2(b) and 2(e). Although our peptide is much larger, we see in line with previous results for alanine dipeptide[14] that the relaxation times of all three components χ_{PP}, χ_{HP}, and χ_{OP} shown in Figure 5 are very similar and given by roughly $\tau \approx 700$ ps (see Table I for the explicit fitting results). In simulations of lysozyme, the relaxation times of the PP and the water-peptide (WP) processes were found to significantly differ from each other and a fast water-like relaxation process was seen in the PP as well as in the WP contributions,[16] quite different from our results, which points to protein-specific effects that will be discussed further below. A closer look at the amplitudes in Figure 5 reveals that the peptide auto-correlation term χ_{PP} dominates over the cross terms χ_{HP} and χ_{OP}. Interestingly, the

peptide-outer shell water cross term χ_{OP} exceeds the peptide-hydration water cross term χ_{HP} by roughly a factor of two, meaning that the peptide correlates less with the first hydration shell than with the remaining water. In fact, increasing the hydration shell radius from $R_H = 3$ Å to $R_H = 6$ Å enhances the peptide-hydration-water cross term contribution by less than 20% from $\chi'_{HP}(f = 0) = 0.69$ to $\chi'_{HP}(f = 0) = 0.82$, as shown in Table IV. This rather weak correlation between the peptide and the second hydration shell motivated our choice of a relatively small hydration shell radius of $R_H = 3$ Å. As a comparison of the last two rows of Table IV demonstrates,

TABLE IV. Effect of the definition of the hydration shell radius R_H on the static contribution of the peptide-hydration water cross correlation contribution $\chi'_{HP}(f = 0)$. We also show the average number of hydration shell water molecules N_H and the hydration water fraction $n_H = N_H/N$. More than one third of the cross term contribution is caused by the first hydration shell with a radius $R_H = 3$ Å. On the other hand, 30% of the contribution comes from water molecules which are more than 1 nm away from the peptide. Note that with the exception of Figure 6, all spectra shown in this work are obtained using a fixed hydration radius $R_H = 3$ Å.

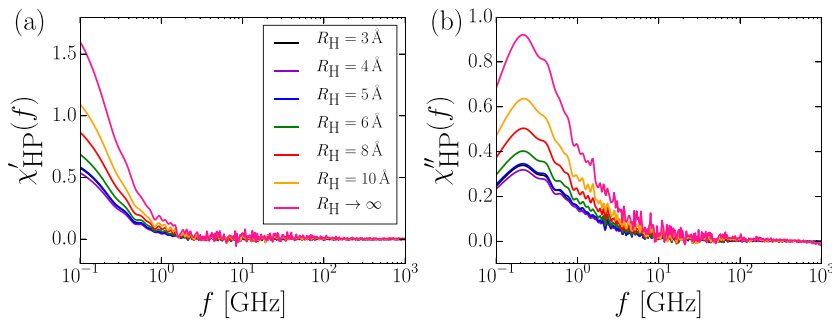| R_H (Å)	$\chi'_{HP}(f = 0)$	N_H	n_H
3	0.69	34.7	0.051
4	0.64	82.9	0.121
5	0.70	119.1	0.173
6	0.82	172.3	0.250
7	0.91	232.8	0.338
8	1.04	296.9	0.432
9	1.17	364.4	0.530
10	1.31	434.5	0.632
∞	1.91	688.0	1.000

FIG. 6. Comparison of the real (a) and imaginary (b) parts of the peptide-hydration-water cross correlation χ_{HP} for various hydration shell radii R_H. Note that the data for $R = 3$ Å (black line) and for $R = 5$ Å (blue line) are almost identical and that an infinite hydration radius encompasses all water, i.e., $\chi_{HP} = \chi_{WP}$ for $R_H \to \infty$.

about 30% of the peptide-water cross-contribution $\chi'_{WP}(f = 0)$ is caused by water molecules that are more than 1 nm away from the peptide, demonstrating the long range of peptide-water polarization correlations. This finding agrees nicely with the conclusions from protein-concentration dependent THz absorption studies[3,4] and simulation studies of aqueous solutions of larger peptides.[16,28] The peptide-hydration-water cross term contribution $\chi_{HP}(f)$ is shown for various hydration radii R_H in Figure 6, one sees that the amplitude continuously increases with growing radius, while the spectral shape stays rather invariant.

The folding state of the peptide has a small but systematic influence on the peptide polarization relaxation time, one observes a slight blue shift for all three contributions χ_{PP}, χ_{HP}, and χ_{OP} in Figure 5 from the folded (blue lines) to the unfolded state (green lines). The relaxation time of the Cole-Cole fits for χ_{PP} decreases by about 35% from the folded state, $\tau = 734$ ps, to the unfolded state, $\tau = 550$ ps, see Table I.

The polarization relaxation of peptides is typically associated with the rotational relaxation time. In Figure 4(d) (black line), we show that the auto-correlation of the end-to-end vector $\vec{R}_{ee}(t)$ between the C_α atoms of the first and last alanine monomers decays exponentially with a decay time of $\tau_R = 832$ ps, quite close to the χ_{PP} relaxation time of the entire trajectory of $\tau = 719$ ps. The end-to-end unit vector $\vec{R}_{ee}(t)/|\vec{R}_{ee}(t)|$ (blue line) shows a somewhat shorter relaxation time of $\tau_r = 779$ ps, while the magnitude of the end-to-end vector $|\vec{R}_{ee}(t)| - \langle|\vec{R}_{ee}|\rangle$ (green line) exhibits an intermediate relaxation time of $\tau_{|R|} = 813$ ps. Based on the good match between polarization and orientational relaxation times, we conclude that peptide polarization correlations are indeed caused by orientational correlations, in agreement with common notions. To further understand this coupling, we next compare the simulated peptide rotational relaxation time with a simple model based on the rotational motion of a cylinder of length L and radius R in a viscous solvent. The rotational diffusion constant D_{rot} to first order in the characteristic ratio R/L is given by[38]

$$D_{rot} = \frac{3k_B T}{\pi L^3 \eta} \left(\ln(L/R) - 1.57 + 7(1/(\ln(L/R)) - 0.28)^2 \right).$$

Using for the dynamic viscosity of SPC/E water $\eta = 6.8 \times 10^{-4}$ N/(m s)[39] and for the radius and the length of an ideal α-helix based on the backbone carbon atom positions $R = 0.23$ nm and $L = 1.2$ nm (0.15 nm per monomer), we obtain $\tau_{rot} = 1/(2D_{rot}) = 181$ ps, which is by a factor four lower than that found in the simulations. If the presence of side-

chains and end-caps is included by increasing the characteristic lengths to $L = 1.5$ nm and $R = 0.33$ nm (note that increasing the radius R decreases the rotational relaxation time τ_{rot}), we predict $\tau_{rot} = 303$ ps, still too low. Note that a further increase of the cylinder length to $L = 1.9$ nm would be needed to reproduce the simulation results for the orientational relaxation time based on the model of a stiff cylinder. We conclude that such a length is not completely unrealistic, but at the same time mention that internal dissipative modes due to the finite peptide flexibility are expected to cause deviations between the simple model and the more realistic simulation results for the rotational relaxation time, in particular in the unfolded state.

In line with the above reasoning, an even slower polarization relaxation time of about 2.5 ns was reported for the 76-residue protein ubiquitin,[40] which confirms that orientational and polarization relaxation times are correlated.

D. Water contribution

In Sec. III C, we focused on the effect the peptide secondary structure has on spectral contributions involving the peptide polarization, including peptide-water cross terms. In this section, we investigate how the peptide folding state influences the polarization correlations between water molecules themselves. For that, we decompose the water-water auto-correlation contribution further as $\chi_{WW} = \chi_{HH} + \chi_{OO} + 2\chi_{HO}$ into hydration water autocorrelations χ_{HH}, outer shell water autocorrelations χ_{OO}, and hydration-outer shell cross correlations χ_{HO}, analogously to Boresch et al.[14] We extend their decomposition by an additional projection into folded and unfolded states.

For the outer shell water dielectric response χ_{OO} in Figures 7(b) and 7(e), an impact of the peptide folding state is not observable, the spectrum is perfectly described by a Cole-Cole fit with small exponent $\alpha < 0.02$ (see Table I) close to pure bulk water,[37] meaning that the peptide has virtually no influence on the outer shell water, neither in the folded nor in the unfolded state. This is even more remarkable, considering our very thin definition of the hydration shell.

In contrast, the spectral contributions involving hydration waters χ_{HH} and χ_{HO} show features in the sub-GHz range which are more pronounced in the folded state. The amplitudes of the χ_{HH} and χ_{HO} contributions are larger in the unfolded state (green lines) compared to the folded state (blue lines), which reflects the rather trivial fact that the number fraction of hydration shell water in the unfolded state is $n_H = 5.68\%$ and thus slightly larger than the corresponding number in the
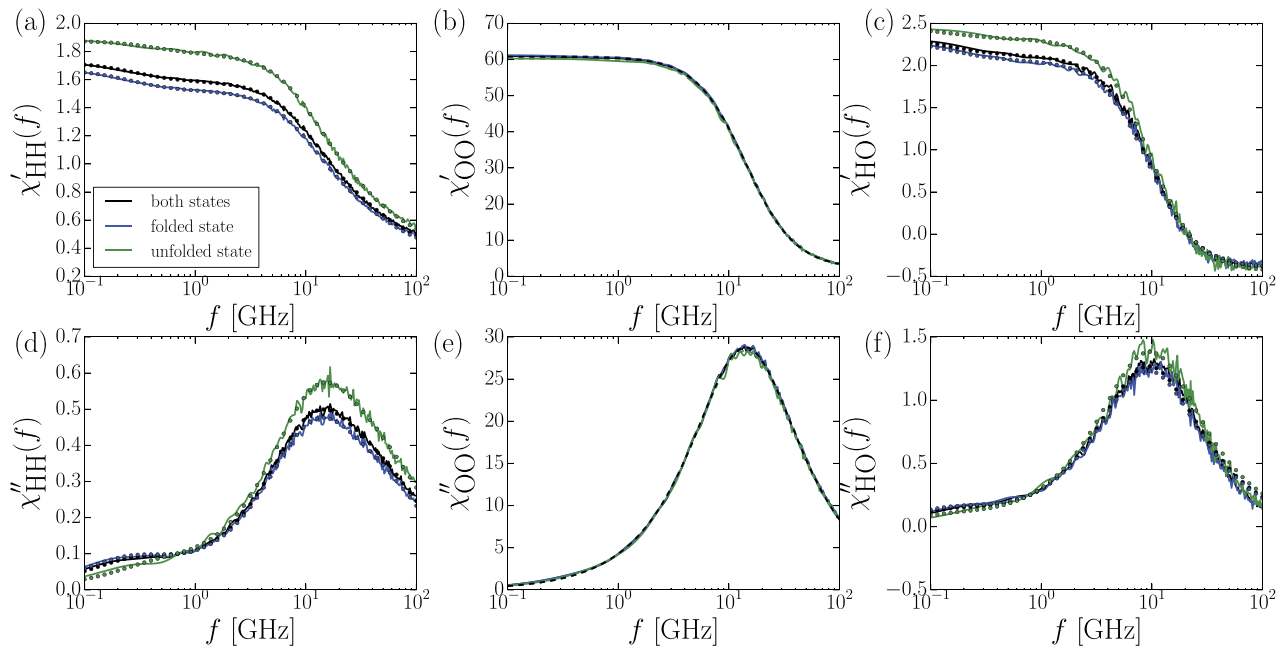
FIG. 7. Real (a) and imaginary (d) parts of the hydration-water dielectric susceptibility $\chi_{HH}(f)$ for the folded state (blue), the unfolded state (green), and for the entire trajectory (black lines). The outer shell-water dielectric susceptibility $\chi_{OO}(f)$ (b) and (e) does not depend on the peptide state. The signal due to hydration-water-outer shell water cross correlations $\chi_{HO}(f)$ (c) and (f) is slightly larger for an unfolded peptide and the relaxation is slightly slower than for HH and OO. Triple Debye fits are shown for χ_{HH} as dotted lines, while Cole-Cole fits (dashed lines) are almost indistinguishable from the data for χ_{OO}. Double Debye fits are shown for χ_{HO} as dotted lines.

unfolded state $n_H = 4.84\%$ (the average over the entire trajectory including folded and unfolded states yields 5.05%). Note that for very high frequencies, the absorption spectrum $\chi''_{HO}(f)$ is significantly negative, while $\chi''_{HH}(f)$ exhibits the opposite trend. This spurious behavior is due to water molecules that leave and reenter the hydration shell at high frequency and will not be discussed further.

In line with earlier theoretical results on single-alanine and di-alanine[14] and NAGMA and NALMA,[41] we find that the cross term χ_{HO} is significantly slower ($\tau \approx 17.5$ ps) than the χ_{HH} and χ_{OO} contributions (τ approximately 9 and 11 ps, Table I). As a matter of fact, this behavior is not so much a characteristic feature of hydration water but rather trivially follows from the different nature of self and collective

polarization contributions: it is well-known that the self relaxation of water is faster than the collective relaxation in pure water as well as in ionic solutions.[42–44] Neglecting the rather infrequent interchange of individual water molecules between the hydration and outer shell ensembles, the cross term χ_{HO} only consists of collective relaxations, i.e., $\chi_{HO}(f) \approx \chi_{HO,coll}(f)$. In contrast, the contributions χ_{HW} and χ_{OW} consist of self and collective terms, as defined in Eqs. (34) and (35), analogously to our recent work on ionic solutions.[37] A direct comparison of self and collective parts of χ_{HO}, χ_{HW}, and χ_{OW} is shown in Figure 8, where the much larger χ_{OW} contribution is rescaled by a factor 0.1. Figure 8(b) demonstrates that the three collective parts χ_{HO} (black), $\chi_{HW,coll}$ (green), and $\chi_{OW,coll}$ (orange) have almost identical relaxation times, while
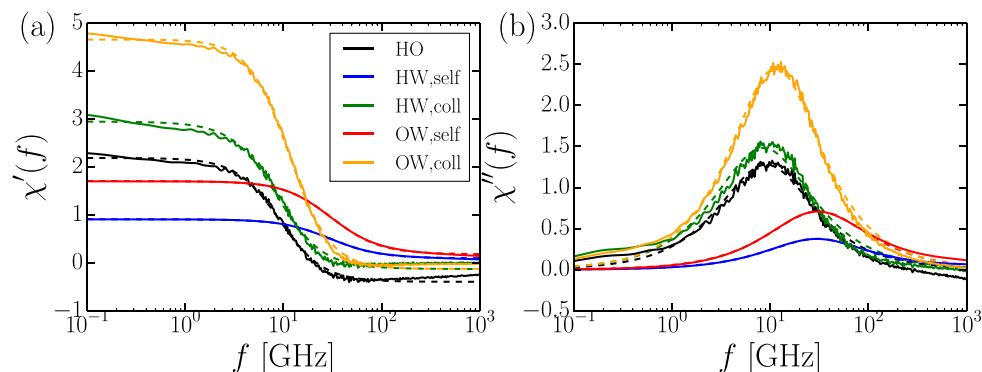

FIG. 8. Comparison of different components of the real (a) and imaginary (b) parts of the water susceptibilities: the outer shell-hydration water cross correlation contribution $\chi_{HO}(f)$ (black line) and the collective hydration water $\chi_{HW,coll}$ (green line) and the collective outer shell water $\chi_{OW,coll}$ contributions (orange line) occur on roughly the same time scale. The self hydration water $\chi_{HW,self}$ (blue line) and the self outer shell water contributions $\chi_{OW,self}$ (red line) are much faster than the collective relaxations. The dashed lines are Cole-Cole fits. The bulk contributions $\chi_{OW,coll}$ and $\chi_{OW,self}$ (orange and red lines) have been decreased by one order of magnitude for better comparison.
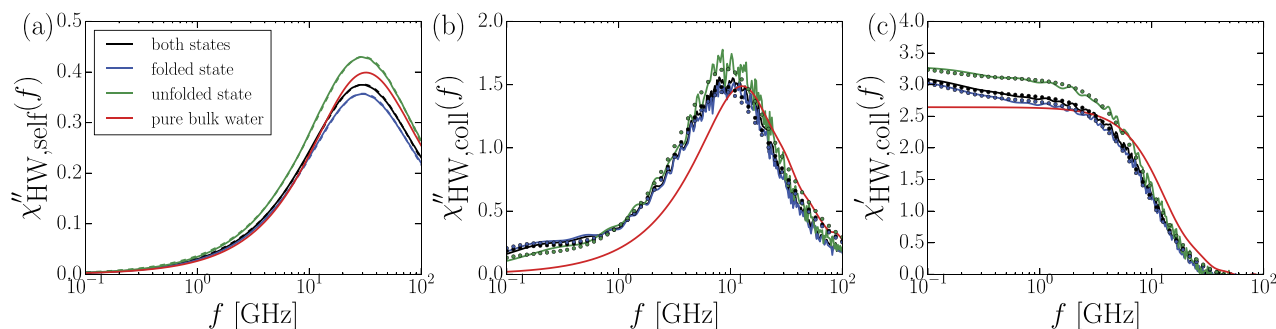
FIG. 9. (a) Imaginary part of the self relaxation of the hydration shell water for the folded state (blue), the unfolded state (green), and for the entire trajectory (black line), in comparison with the self-relaxation spectrum of pure water (red line). The spectra are slightly red-shifted compared to pure water and well described by Cole-Cole fits (dashed lines). In the unfolded state, the amplitude is slightly higher due to the increased number of hydration water molecules. (b) Imaginary part of the collective spectral contribution due to hydration shell water: In particular in the folded state, the spectrum has a second peak in the sub-GHz range. Double Debye fits reproduce the spectral shape well (dotted lines). The high-frequency peak is slightly red-shifted compared to the collective contribution of pure water (red line). (c) Real part of the collective dielectric contribution of hydration shell water, the static contribution is slightly higher than in pure water (red line). The dielectric spectra of the self and collective parts of pure water (red lines) are multiplied with a factor of 0.05 in all subfigures in order to account for the small hydration water fraction in the peptide simulation.

the two self contributions $\chi_{HW,self}$ (blue) and $\chi_{OW,self}$ (red) are significantly faster; the fit parameters in Table I support this graphical impression. The HO relaxation time $\tau = 17.5$ ps is situated between the faster OW collective relaxation time $\tau = 14.0$ ps and the slightly slower collective HW relaxation time $\tau = 18.6$ ps. We conclude that the slow relaxation time of the cross term χ_{HO} with $\tau = 17.5$ ps compared to the hydration water contribution χ_{HH} with $\tau = 9.2$ ps and the outer-shell water contribution χ_{OO} with $\tau = 11.3$ ps is due to the generally slow collective water relaxation and not related to any particular properties of hydration water.

Since the cross-contribution χ_{HO} ($\tau = 17.5$ ps, Table I) is only 25% slower than the collective relaxation $\chi_{OW,coll}$, $\tau = 14.0$ ps, we do not think that this term can be associated with the intermediate time scale δ-process seen in some experiments. Similarly, although a triple-Debye fit is necessary to accurately describe the spectral shape of χ_{HH} in Figures 7(a) and 7(d), it is also unlikely that χ_{HH} is related to the δ-process. In the decomposition $\chi_{WW} = \chi_{HH} + 2\chi_{HO} + \chi_{OO}$, the auto-correlation term χ_{HH} contains disproportionately more self-relaxation contributions in comparison with χ_{WW}. So the fast peak in the triple-Debye fit to χ_{HH} ($\tau = 2.9$ ps in Table IV) reflects self-relaxations, and the intermediate peak ($\tau = 13.2$ ps) reflects collective contributions, similar to pure water where we found that the decomposition of the single Debye-like pure water signal with $\tau = 10.7$ ps into self and collective processes leads to two processes with Cole-Cole relaxation times of $\tau = 4.3$ and $\tau = 13.0$ ps[37] (see Table I). The slowest process of the triple Debye fit to χ_{HH} with $\tau = 578$ ps again is rather close to the peptide polarization relaxation time of about 700 ps, and it seems unlikely that this contribution could be resolved as a separate peak in experimental spectra.

The spectral contributions χ_{HH} and χ_{HO} in Figures 7(d) and 7(f) show a slow process and a weak secondary structure dependence. In order to further investigate these effects, the self and collective contributions of the combined signal $\chi_{HW} = \chi_{HH} + \chi_{HO}$ are compared in Figure 9. We use χ_{HW} instead of χ_{HH} to omit effects of water molecules that leave and reenter the hydration shell at high frequency. The self relaxation in Figure 9(a) (green line) has a higher amplitude in the unfolded

state because of the earlier-mentioned larger number of hydration water molecules in the unfolded state. Independent of the secondary structure, the self relaxation peak is slightly red-shifted compared to the spectrum for pure bulk water (red line, shifted down by a factor 0.05 to account for the small number of hydration water molecules) and well described by a Cole-Cole process. To give explicit numbers, the self-relaxation time of hydration shell water is $\tau = 5.24$ ps and $\tau = 5.25$ ps in the folded and unfolded states, respectively, and thus only slightly larger than the self-relaxation of bulk water $\tau = 4.3$ ps which we obtained from separate simulations (see Table I). This and the absence of additional slow spectral features show that individual water dipoles reorient in an almost unhindered manner even close to the peptide. Note that a much more pronounced slowing down of the water self relaxation in the first hydration shell was found in previous simulations of ubiquitin and plastcyanin,[45,46] which suggests that the hydration water orientational dynamics is strongly dependent on the protein type.

In contrast, a slow process appears in the collective relaxation $\chi_{HW,coll}$ in Figure 9(b) and is more pronounced in the folded state (blue line). $\chi_{HW,coll}$ cannot be well described by a single Cole-Cole fit (not shown), only a double Debye fit reproduces the spectral shape and is shown by dotted lines. The relaxation time of the slower process in the double Debye fit exceeds 1 ns and is almost independent of the secondary structure while the amplitude of the slow peak ϵ_1 decreases from 0.38 for the folded state to 0.20 for the unfolded state (Table II). The high-frequency main peak extends to lower frequencies compared to the rescaled collective absorption signal of pure bulk water taken from our previous work,[37] which is multiplied with the average hydration water fraction n_H of 0.05 to allow for a meaningful comparison of the spectra (red line, Figure 9(b)). We conclude that mostly the collective part of the hydration water spectral contribution is influenced by the presence of the peptide, and even here, the impact is rather small, in agreement with previous theoretical findings.[10]

Due to the additional slow processes, the static dielectric contribution of the hydration-water collective relaxations in Figure 9(c) is about 20% higher than the collective contribution of the same amount of pure water, which is shown by a red line.

At the same time, the signal is slightly red-shifted compared to pure water, as can be seen in Figure 9(b). The combination of an increased dielectric constant with an increased relaxation time for hydration water is opposite to the trends seen for the hydration water in most electrolyte solutions. For instance, sodium-halide solutions exhibit a dielectric decrement and accelerated collective water dynamics compared to pure bulk water.[37] Nevertheless, the linear correlation between dielectric constant and relaxation time is perfectly in line with the Madden-Kivelson-Equation,[47] which rationalizes this in terms of collective many-body correlation effects. In essence, the dielectric contribution of hydration water is larger than a comparable amount of bulk water, and the relaxation dynamics is slowed down because the peptide enhances the collective water polarization correlations in its hydration shell, a peptide acts as a dielectric structure maker (in contrast to ionic solutions which typically act as dielectric structure breakers[37]).

IV. CONCLUSIONS

Via projection of the simulation trajectory into sections corresponding to folded and unfolded states, we show that the dielectric spectrum of a single Ala_8 peptide chain in water is significantly impacted by the presence of the helical secondary structure, especially in the sub-GHz range. If the peptide is helical, the static dielectric constant is higher and the low-frequency absorption is increased compared to the unfolded state. By a further decomposition, we show that the secondary structure mainly affects the spectral contributions involving the peptide polarization. In line with previous work, we find that hydration water exhibits a low frequency dielectric contribution at a similar time scale as the peptide itself, but this low-frequency contribution is mostly due to peptide-hydration water polarization correlations and not so much due to hydration water-hydration water auto-correlations. In fact, our further decomposition of the water polarization correlations into self and collective molecular relaxations demonstrates that the sub-GHz absorption of hydration water is a purely collective phenomenon. This means the studied peptide Ala_8 hinders the orientational relaxation of single water molecules only slightly (when projected along their dipolar axis). On the other hand, we do not see any traces of fast polarization dynamics in the peptide contribution in the 10 GHz range where bulk water shows its main relaxation dynamics, not even in the peptide-water cross correlations. Our findings are interesting in light of the picture of "slaving water" around proteins, according to which solvent fluctuations control the protein dynamics.[1,2,48] We only find a "slaved hydration shell" where the observed collective polarization processes in the hydration shell follow the slow peptide reorientational dynamics, while individual water molecules are nevertheless free to reorient almost as quickly as in bulk. In contrast, in simulations of lysozyme, faster peptide relaxation processes have been found.[16] This could mean that the dynamic slaving influence of water on peptides is quite specific and depends on the presence of certain protein features. In this respect, it is interesting to note that our used alanine polypeptide has no hydrophilic side chains, which might be necessary for water

to couple dynamically to a peptide in the GHz range. This is a possibility worth following up in the future.

The slaving-water concept is partly based on the similar temperature dependences of the dielectric relaxation time of water in the GHz range and protein relaxation processes occurring at frequencies that are smaller by two orders of magnitude.[1] The absence of a dynamic coupling between hydration water and peptide at the dominant water relaxation frequency around 10 GHz, which we observe in our simulations for Ala_8 might suggest that the dynamic cross talk between protein and hydration water is more indirect and involves the interplay between solvent and internal viscosity effects, as was previously concluded from experimental studies[49] and recently confirmed theoretically.[50] On the other hand, it is interesting to note that a quite strong dynamic peptide-hydration water coupling in the THz regime has been observed in recent simulations,[15] but the connection of this THz coupling to the peptide dynamics at much smaller frequencies is not clear.

The influence the peptide has on the slow collective relaxation dynamics of hydration water is quite long-ranged, 30% of the peptide-hydration water cross correlations extends by more than 1 nm into the water phase. The at first view astonishingly slow relaxation of the hydration-outer shell water cross-contribution noticed in earlier publications is explained in terms of the dominance of collective terms, which are generically slower than water self-correlations.

Our results do not contain a statistically significant δ-process in addition to the common bulk water peak around 10 GHz and a slow peak around 200 MHz mainly caused by the peptide reorientation dynamics. The small differences of the relaxation times we obtain for different components via decomposition makes the assignment of intermediate processes challenging and prone to failure. In the future, it would be interesting to redo similar simulations with larger peptides that would consequently exhibit slower peptide relaxation times and to see whether in between the peptide and bulk water relaxation times, an intermediate relaxation process can be clearly established. In light of the long simulation time of 7 μs we needed in order to reach sufficient statistics, this will be challenging from a computational point of view. In reverse, it would be desirable to have access to experimental spectra for Ala_8 solutions or similar-sized peptides in order to compare with simulation results.

Because of simulation time constraints, we only studied a single peptide embedded in water; in the future and in order to more meaningfully compare with experiments, it would be important to extend the current study to include many-peptide effects. We believe that the force field quality is a rather minor issue, since we validated various force fields and in particular our simulation technology previously for electrolyte solutions, where we found good agreement between simulated dielectric spectra and experimental results even for the quite subtle ion-specific effects.[37]

The folding/unfolding transition itself will of course also lead to a dielectric contribution with a frequency of the order of the inverse folding time, because the peptide polarization in the folded and unfolded states is quite different. In future experimental and theoretical studies, it would be interesting to follow up on such effects in more detail.

ACKNOWLEDGMENTS

[1]P. W. Fenimore, H. Frauenfelder, B. H. McMahon, and F. G. Parak, "Slaving: Solvent fluctuations dominate protein dynamics and functions," PNAS **99**(25), 16047–16051 (2002).

[2]H. Frauenfelder, G. Chen, J. Berendzen, P. W. Fenimore, H. Jansson, B. H. McMahon, I. R. Stroe, J. Swenson, and R. D. Young, "A unified model of protein dynamics," PNAS **106**(13), 5129–5134 (2009).

[3]S. Ebbinghaus, S. J. Kim, M. Heyden, X. Yu, U. Heugen, M. Gruebele, D. M. Leitner, and M. Havenith, "An extended dynamical hydration shell around proteins," PNAS **104**(52), 20749–20752 (2007).

[4]B. Born, S. J. Kim, S. Ebbinghaus, M. Gruebele, and M. Havenith, "The terahertz dance of water with the proteins: The effect of protein flexibility on the dynamical hydration shell of ubiquitin," Faraday Discuss. **141**, 161–173 (2009).

[5]C. Grosse and A. V. Delgado, "Dielectric dispersion in aqueous colloidal systems," Curr. Opin. Colloid Interface Sci. **15**(3), 145–159 (2010).

[6]M. Wolf, R. Gulich, P. Lunkenheimer, and A. Loidl, "Broadband dielectric spectroscopy on human blood," Biochim. Biophys. Acta **1810**(8), 727–740 (2011).

[7]N. Miura, Y. Hayashi, N. Shinyashiki, and S. Mashimo, "Observation of unfreezable water in aqueous solution of globule protein by microwave dielectric measurement," Biopolymers **36**(1), 9–16 (1995).

[8]C. Cametti, S. Marchetti, C. M. C. Gambi, and G. Onori, "Dielectric relaxation spectroscopy of lysozyme aqueous solutions: Analysis of the δ-dispersion and the contribution of the hydration water," J. Phys. Chem. B **115**(21), 7144–7153 (2011).

[9]H. P. Schwan, "Electrical properties of blood and its constitutents: Alternating current spectroscopy," Blut **46**(4), 185–197 (1983).

[10]A. Oleinikova, P. Sasisanker, and H. Weingärtner, "What can really be learned from dielectric spectroscopy of protein solutions? A case study of ribonuclease A," J. Phys. Chem. B **108**(24), 8467–8474 (2004).

[11]A. Knocks and H. Weingärtner, "The dielectric spectrum of ubiquitin in aqueous solution," J. Phys. Chem. B **105**(17), 3635–3638 (2001).

[12]P. Sasisanker and H. Weingärtner, "Hydration dynamics of water near an amphiphilic model peptide at low hydration levels: A dielectric relaxation study," ChemPhysChem **9**(18), 2802–2808 (2008).

[13]I. Rodríguez-Arteche, S. Cerveny, Á. Alegría, and J. Colmenero, "Dielectric spectroscopy in the GHz region on fully hydrated zwitterionic amino acids," PCCP **14**(32), 11352–11362 (2012).

[14]S. Boresch, M. Willensdorfer, and O. Steinhauser, "A molecular dynamics study of the dielectric properties of aqueous solutions of alanine and alanine dipeptide," J. Chem. Phys. **120**(7), 3333–3347 (2004).

[15]M. Heyden and M. Havenith, "Combining THz spectroscopy and MD simulations to study protein-hydration coupling," Methods **52**(1), 74–83 (2010).

[16]D. V. Matyushov, "Dipolar response of hydrated proteins," J. Chem. Phys. **136**(8), 085102 (2012).

[17]D. R. Martin and D. V. Matyushov, "Dipolar nanodomains in protein hydration shells," J. Phys. Chem. Lett. **6**(3), 407–412 (2015).

[18]S. Bone, "Dielectric studies of native, unfolded and intermediate forms of beta-lactamase," Phys. Med. Biol. **39**(11), 1801 (1994).

[19]Y. Hayashi, Y. Katsumoto, S. Omori, N. Kishii, and A. Yasuda, "Liquid structure of the urea-water system studied by dielectric spectroscopy," J. Phys. Chem. B **111**(5), 1076–1080 (2007).

[20]A. Idrissi, M. Gerard, P. Damay, M. Kiselev, Y. Puhovsky, E. Cinar, P. Lagant, and G. Vergoten, "The effect of urea on the structure of water: A molecular dynamics simulation," J. Phys. Chem. B **114**(13), 4731–4738 (2010).

[21]M. Wolf, R. Gulich, P. Lunkenheimer, and A. Loidl, "Relaxation dynamics of a protein solution investigated by dielectric spectroscopy," Biochim. Biophys. Acta **1824**(5), 723–730 (2012).

[22]U. Kaatze, "Complex permittivity of water as a function of frequency and temperature," J. Chem. Eng. Data **34**(4), 371–374 (1989).

[23]R. Buchner, J. Barthel, and J. Stauber, "The dielectric relaxation of water between 0 °C and 35 °C," Chem. Phys. Lett. **306**(1), 57–63 (1999).

[24]A. S. Reddy, L. Wang, Y.-S. Lin, Y. Ling, M. Chopra, M. T. Zanni, J. L. Skinner, and J. J. De Pablo, "Solution structures of rat amylin peptide: Simulation, theory, and experiment," Biophys. J. **98**(3), 443–451 (2010).

[25]P. Hamm, J. Helbing, and J. Bredenbeck, "Two-dimensional infrared spectroscopy of photoswitchable peptides," Annu. Rev. Phys. Chem. **59**, 291–317 (2008).

[26]A. L. Serrano, M. J. Tucker, and F. Gai, "Direct assessment of the α-helix nucleation time," J. Phys. Chem. B **115**(22), 7472–7478 (2011).

[27]H. S. Chung and W. A. Eaton, "Single-molecule fluorescence probes dynamics of barrier crossing," Nature **502**, 685–688 (2013).

[28]M. Heyden, D. J. Tobias, and D. V. Matyushov, "Terahertz absorption of dilute aqueous solutions," J. Chem. Phys. **137**(23), 235103 (2012).

[29]M. Heyden and D. J. Tobias, "Spatial dependence of protein-water collective hydrogen-bond dynamics," PRL **111**(21), 218101 (2013).

[30]F. Kohler, G. H. Findenegg, J. Fischer, and H. Posch, *The Liquid State* (Verlag Chemie, Weinheim, 1972).

[31]S. R. De Groot and P. Mazur, *Non-Equilibrium Thermodynamics* (Dover, New York, 1984).

[32]K. F. Rinne, S. Gekle, and R. R. Netz, "Dissecting ion-specific dielectric spectra of sodium-halide solutions into solvation water and ionic contributions," J. Chem. Phys. **141**(21), 214502 (2014).

[33]B. Hess, C. Kutzner, D. van der Spoel, and E. Lindahl, "GROMACS 4: Algorithms for highly efficient, load-balanced, and scalable molecular simulation," J. Chem. Theory Comput. **4**(3), 435–447 (2008).

[34]Y. Duan, C. Wu, S. Chowdhury, M. C. Lee, G. Xiong, W. Zhang, R. Yang, P. Cieplak, R. Luo, and T. Lee, "A point-charge force field for molecular mechanics simulations of proteins based on condensed-phase quantum mechanical calculations," J. Comput. Chem. **24**(16), 1999–2012 (2003).

[35]G. Bussi, D. Donadio, and M. Parrinello, "Canonical sampling through velocity rescaling," J. Chem. Phys. **126**(1), 014101 (2007).

[36]M. Parrinello and A. Rahman, "Polymorphic transitions in single crystals: A new molecular dynamics method," J. Appl. Phys. **52**(12), 7182–7190 (1981).

[37]K. F. Rinne, S. Gekle, and R. R. Netz, "Ion-specific solvation water dynamics: Single water versus collective water effects," J. Phys. Chem. A **118**(50), 11667–11677 (2014).

[38]S. Broersma, "Rotational diffusion constant of a cylindrical particle," J. Chem. Phys. **32**(6), 1626–1631 (1960).

[39]S. Tazi, A. Boţan, M. Salanne, V. Marry, P. Turq, and B. Rotenberg, "Diffusion coefficient and shear viscosity of rigid water models," J. Phys. Condens. Matter **24**(28), 284117 (2012).

[40]S. Boresch, P. Höchtl, and O. Steinhauser, "Studying the dielectric properties of a protein solution by computer simulation," J. Phys. Chem. B **104**(36), 8743–8752 (2000).

[41]R. K. Murarka and T. Head-Gordon, "Dielectric relaxation of aqueous solutions of hydrophilic versus amphiphilic peptides," J. Phys. Chem. B **112**(1), 179–186 (2008).

[42]E. Harder, J. D. Eaves, A. Tokmakoff, and B. J. Berne, "Polarizable molecules in the vibrational spectroscopy of water," PNAS **102**(33), 11611–11616 (2005).

[43]D. Laage and J. T. Hynes, "Reorientional dynamics of water molecules in anionic hydration shells," PNAS **104**(27), 11167–11172 (2007).

[44]G. Stirnemann, E. Wernersson, P. Jungwirth, and D. Laage, "Mechanisms of acceleration and retardation of water dynamics by ions," JACS **135**(32), 11824–11831 (2013).

[45]R. Abseher, H. Schreiber, and O. Steinhauser, "The influence of a protein on water dynamics in its vicinity investigated by molecular dynamics simulation," Proteins **25**(3), 366–378 (1996).

[46]A. R. Bizzarri and S. Cannistraro, "Molecular dynamics of water at the protein-solvent interface," J. Phys. Chem. B **106**(26), 6617–6633 (2002).

[47]P. Madden and D. Kivelson, "A consistent molecular treatment of dielectric phenomena," Adv. Chem. Phys. **56**, 467–566 (1984).

[48]S. Khodadadi, J. H. Roh, A. Kisliuk, E. Mamontov, M. Tyagi, S. A. Woodson, R. M. Briber, and A. P. Sokolov, "Dynamics of biological macromolecules: Not a simple slaving by hydration water," Biophys. J. **98**(7), 1321–1326 (2010).

[49]A. Ansari, C. M. Jones, E. R. Henry, J. Hofrichter, and W. A. Eaton, "Conformational relaxation and ligand binding in myoglobin," Biochemistry **33**(17), 5128–5145 (1994).

[50]J. C. F. Schulz, L. Schmidt, R. B. Best, J. Dzubiella, and R. R. Netz, "Peptide chain dynamics in light and heavy water: Zooming in on internal friction," JACS **134**(14), 6273–6279 (2012).

[51]H. Berendsen, J. Grigera, and T. Straatsma, "The missing term in effective pair potentials," J. Phys. Chem. **91**(24), 6269–6271 (1987).